



Electrocatalysis of oxygen reduction at poly (4-amino-3-hydroxynaphthalene sulfonic acid) and platinum loaded polymer modified glassy carbon electrodes

Berhanu W. Zewde^{*,1}, Shimelis Admassie

Department of Chemistry, Addis Ababa University, P. O. Box 1176, Addis Ababa, Ethiopia

HIGHLIGHTS

- p-(AHNSA) is a new for electrocatalysis of oxygen reduction reaction.
- Electrochemical deposition of platinum metal on p-(AHNSA) is possible.
- It will contribute the research for reducing the amount of platinum.
- It will contribute for attaining the 1 g of platinum/kWh aim.

ARTICLE INFO

Article history:

Received 5 April 2012

Received in revised form

8 June 2012

Accepted 15 June 2012

Available online 23 June 2012

Keywords:

4-Amino-3-hydroxynaphthalene sulfonic acid

Platinum

Oxygen reduction reaction

Glassy carbon electrode

ABSTRACT

The electrochemical polymerization of p-(4-amino-3-hydroxynaphthalene sulfonic acid) is investigated by using cyclic voltammetry. Low amount of platinum is loaded (17–303 µg) on the polymer modified glassy carbon electrode. The electrocatalytic activity of the modified electrodes towards oxygen reduction reaction is investigated. The polymer modified glassy carbon electrode shows a two electron reduction of oxygen to hydrogen peroxide and the platinum loaded polymer modified glassy carbon electrode shows a direct four electron reduction of oxygen to water. The chronocoulometric study of the oxygen reduction reaction shows similar results to those obtained with other techniques. Koutecky–Levich plot analysis is used to predict the mechanism and evaluate the kinetic parameters. Temkin adsorption isotherm is observed for lower platinum loading and Langmuirian for high platinum loading.

© 2012 Elsevier B.V. All rights reserved.

1. Introduction

Proton exchange membrane fuel cell (PEMFC) is a promising power source for electric vehicles and portable devices because of its high conversion efficiency, high power density and low pollution. In PEMFC, the electrochemical reduction of oxygen is the major source for the loss of efficiency and rate limiting step as a result of the complex kinetics and the sluggish nature of the reaction.

Polymers like poly (p-aminobenzene sulfonic acid) [1], and poly(1,8-diaminonaphthalene) [2] modified glassy carbon electrode, and chemically polymerized aniline, pyrrole, thiophene, methylthiophene and poly(3,4-ethylenedioxythiophene) (PEDOT)

on graphite electrode have been studied for this application. They showed catalytic activity to different extent with the exception of PEDOT [3].

Over several years, considerable effort has been devoted to the use of platinum, and several researches have been published in different forms, by partial replacement with other metals, or through the maximization of the catalyst surface area. Many of them indicated platinum as a good catalyst and highly stable in various electrolytes. However, platinum is very expensive for use as a catalyst in fuel cell. For practical applications the amount of platinum has to be reduced to decrease the material cost. Reducing the amount of platinum and getting a better catalytic activity will develop the fuel cell by attaining the 1 g of platinum per kWh aim [4,5].

Microplatinum particles dispersed on conducting polymers such as polyaniline [5–9], polypyrrole [10], p-(o-phenylenediamine) [11], Nafion [12–17], poly(3,4-ethylenedioxythiophene) [18] and others [19] for electrocatalytic applications in oxygen reduction reaction have been studied by reducing the amount of platinum consumed and at the same time improving the

^{*} Corresponding author. Current address: Department of Chemistry, University of Rome "La Sapienza", Piazzale Aldo Moro 5, 00185 Rome, Italy. Tel.: +39 3275551422; fax: +39 0612345678.

E-mail address: berh20042001@yahoo.com (B.W. Zewde).

¹ Permanent address. Tel.: +251 911100253; fax: +251 111234296.

performance of the catalytic activity of the cathode. In addition to the micro platinum particles a number of platinum alloys have been studied [20–24].

To our knowledge, there are no reports on the electrochemical polymerization of 4-amino-3-hydroxynaphthalene sulfonic acid (AHNSA) at glassy carbon rotating disk electrode or micro and nano particles of platinum dispersed on the polymer modified glassy carbon rotating disk electrode (p-(AHNSA)/GCRDE) for use in catalyzing the oxygen reduction reaction in acid solution.

In this work, we describe the synthesis of the p-(AHNSA) to our knowledge, the cheapest material for oxygen reduction, at a glassy carbon electrode through electropolymerization. The electropolymerized p-(AHNSA) was also loaded with platinum in different amounts, ranging from 17 μg to 303 μg , and was used to modify a rotating disc glassy carbon electrode. The modified glassy carbon electrode is used to catalyze the oxygen reduction reaction in 0.5 M H_2SO_4 solution saturated with oxygen. Linear sweep voltammetry, cyclic voltammetry and chronocoulometry were used to elucidate the oxygen reduction reaction and calculate the kinetic parameters for the p-(AHNSA)/GCRDE as well as platinum loaded p-(AHNSA)/GCRDE at different amount of platinum.

2. Experimental

4-Amino-3-hydroxynaphthalene sulfonic acid was purchased from Sigma Aldrich; Hexachloroplatinic acid was purchased from research lab Fine Chem Industries, India and was used as received. Distilled water was used to prepare the supporting electrolyte solution.

Cyclic and linear sweep rotating disc electrode voltammetries were carried out at 25 °C with BASi epsilon Bioanalytical systems. Three electrodes' electrochemical cell was employed in the measurement with Ag/AgCl as reference electrode, Platinum wire as counter electrode. Bare GCRDE with geometric area of 0.0707 cm^2 , p-(AHNSA)/GCRDE or platinum loaded p-(AHNSA)/GCRDE as working electrode. The GCRDE was polished with 1.0, 0.3 and 0.05 μm alumina successively and activated in 0.5 M H_2SO_4 solution between +0.8 and –0.8 V.

Electropolymerization of 2 mM AHNSA solution in 0.1 M HNO_3 at the activated GCRDE was carried out using cyclic voltammetry by scanning the potential between –0.8 V and +2.0 V (all potentials are with respect to Ag/AgCl reference electrode) at a scan rate of 100 mV s^{-1} for 16 cycles [25]. Then, the modified electrode was stabilized for 24 cycles in monomer free 0.5 M H_2SO_4 until a steady state is obtained. The platinum loaded p-(AHNSA)/GCRDE was prepared by the electrodeposition of various amounts of platinum (17–303 μg) at a constant electrode potential of –0.150 V in 0.5 M H_2SO_4 solution containing 2 mM $\text{H}_2\text{PtCl}_6 \cdot 6\text{H}_2\text{O}$ and the amount of platinum deposited was calculated by the amount of charge consumed, assuming all the amount of charges consumed are used to reduce platinum (IV) to platinum (0).

The oxygen reduction current on the polymer and platinum loaded polymer was recorded in oxygen saturated 0.5 M H_2SO_4 solution at a sweep rate of 10 mV s^{-1} between +1.0 V and –0.025 V at various rotational speeds. The reduction current was normalized to the geometric area of the electrode ($A = 0.0707 \text{ cm}^2$) and corrected the background electrode current recorded in pure argon saturated 0.5 M H_2SO_4 .

3. Results and discussion

3.1. Characterization of p-(AHNSA) and the platinum deposition

AHNSA in 0.1 M HNO_3 is electropolymerized on a polished glassy carbon rotating disc electrode at a scan rate of 100 mV s^{-1} for

16 cycles between –0.8 V and +2.0 V (Fig. 1). The inset in Fig. 1 shows the cyclic voltammogram of the polymer modified electrode in a monomer free 0.5 M H_2SO_4 supporting electrolyte between –0.8 V and +0.8 V at a scan rate of 100 mV s^{-1} after 24 cycles of stabilization.

During the first cycle, two oxidative and one reductive peaks appear at about +0.23, +0.65 and –0.30 V, respectively. In the consecutive scans, two new additional peaks, appear at about +0.03 and –0.14 V, respectively. With increasing number of cycles, the peak currents for all the peaks increase except for the anodic peak at +0.65 V. This increase in the peak currents with increasing number of cycles indicates the formation of a polymer film on the surface of the GCRDE. These peaks are well resolved in monomer free p-(AHNSA) in 0.5 M H_2SO_4 shown in the inset in Fig. 1 [25].

The effective surface area of the polymer modified electrode is estimated based on its electrochemical response for 10 mM of $\text{K}_3\text{Fe}(\text{CN})_6$ in 1.0 M KNO_3 at different scan rates. It is calculated using the Randles–Svick equation, by plotting I_p vs. $\nu^{1/2}$ (Fig. 2).

$$I_p = 2.69 \times 10^5 ACD^{1/2} n^{3/2} \nu^{1/2} \quad (1)$$

where A is effective electrode area, ν is scan rate, C is $10 \times 10^{-3} \text{ mol L}^{-1}$, D is $7.60 \times 10^{-6} \text{ cm}^2 \text{ s}^{-1}$, n is 1 [26]. The effective electrode area is calculated to be 0.066 cm^2 which is comparable to the electrode geometric area ($A = 0.0707 \text{ cm}^2$).

3.2. Oxygen reduction

3.2.1. Cyclic voltammetry

The inset in Fig. 3 shows the voltammograms of Ar saturated (a) and oxygen saturated (b) 0.5 M H_2SO_4 solution at p-(AHNSA)/GCRDE at a scan rate of 100 mV s^{-1} . In the cyclic voltammogram of the oxygen saturated 0.5 M H_2SO_4 , a new peak started to appear at about –0.34 V and the cathodic peak potential is obtained at about –0.45 V which clearly shows the p-(AHNSA) has electro-catalytic activity towards oxygen reduction reaction.

In Fig. 3, the cyclic voltammograms of platinum loaded p-(AHNSA)/GCRDE in oxygen saturated 0.5 M H_2SO_4 solution at different platinum loading are shown. The current values are

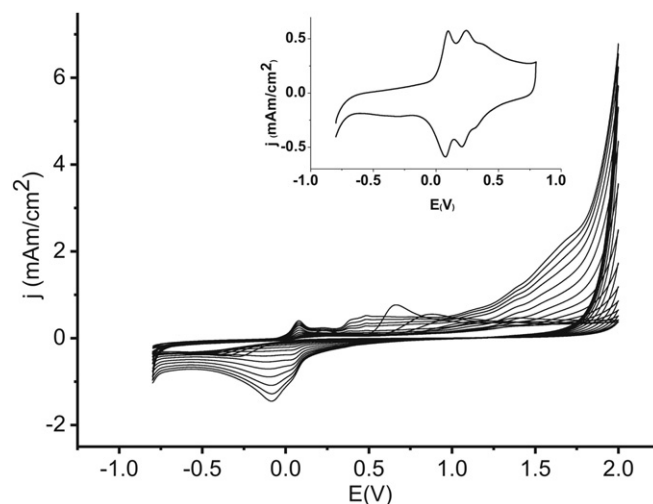


Fig. 1. Cyclic voltammograms recorded during the electropolymerization of 2 mM AHNSA in 0.1 M nitric acid at GCRDE. Scanning potential: –0.8 to +2.0 V; scanning cycles: 16. Inset: cyclic voltammogram of the polymer modified GCRDE in a monomer free 0.5 M H_2SO_4 supporting electrolyte after its stabilization for 24 cycles. Scanning potential: –0.8 to +0.8 V; scan rate: 100 mV s^{-1} .

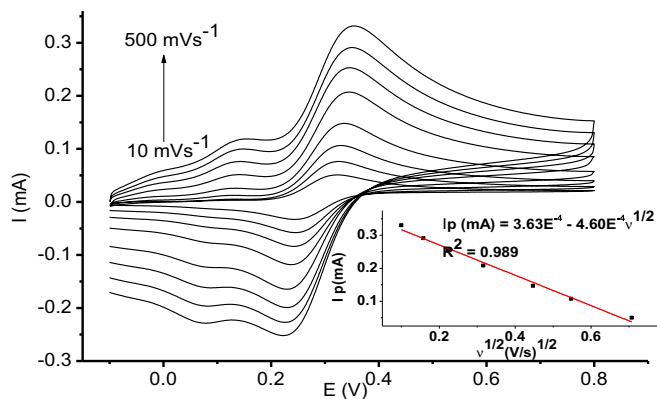


Fig. 2. Cyclic voltammetric response of 10.0 mM $\text{Fe}(\text{CN})_6^{3-}$ in 1 M KNO_3 at the p-(AHNSA)/GCRDE at scan rates of 10, 25, 50, 100, 200, 300, 400, and 500 mV s^{-1} .

normalized with respect to the geometric area of the electrode ($A = 0.0707 \text{ cm}^2$) [23,27]. The potential for the hydrogen adsorption/desorption region is $<0.176 \text{ V}$. As can be seen from the voltammograms, the hydrogen adsorption/desorption current increased with increasing platinum loading illustrating utilization of Pt [23].

The peak potential shift towards positive direction and enhancement of the normalized current of oxygen reduction with increasing platinum loading indicate the catalytic activity of platinum towards oxygen reduction reaction [11].

3.2.2. Chronocoulometry

Fig. 4A shows the double potential-step chronocoulomograms recorded for p-(AHNSA)/GCRDE in oxygen saturated p-(AHNSA)/GCRDE (4A-a) and argon saturated (4A-b) 0.5 M H_2SO_4 solution with an initial and final potentials of +0.5 and -0.8 V . In a similar manner, Fig. 4B represents the double potential-step chronocoulomograms recorded for 181 μg platinum loaded p-(AHNSA)/GCRDE in oxygen saturated (4B-a) and argon saturated (4B-b) 0.5 M H_2SO_4 solution with an initial and final potentials of +0.8 and -0.025 V . The number of electrons is calculated from the charge obtained using Cottrell's equation [28]:

$$Q = \frac{2nFAD^{1/2}C_0t^{1/2}}{\pi^{1/2}} \quad (2)$$

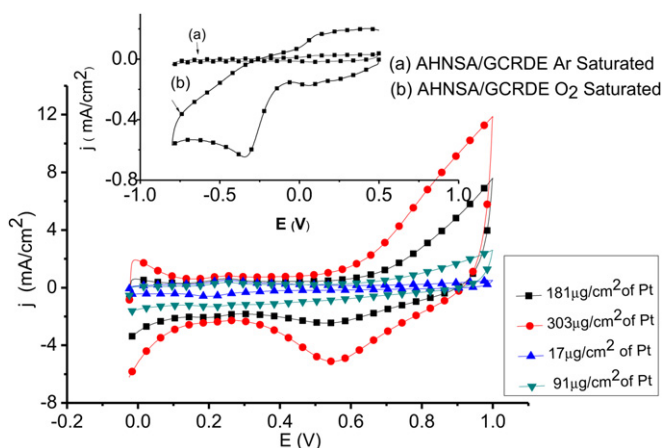


Fig. 3. Cyclic voltammograms for the reduction of oxygen saturated in 0.5 M H_2SO_4 at a p-(AHNSA)/GCRDE with various loadings (17, 91, 181 and 303 $\mu\text{g Pt cm}^{-2}$). Inset: cyclic voltammograms of p-(AHNSA)/GCRDE in (a) Ar saturated and (b) oxygen saturated 0.5 M H_2SO_4 at a scan rate of 100 mV s^{-1} and at 25 $^\circ\text{C}$.

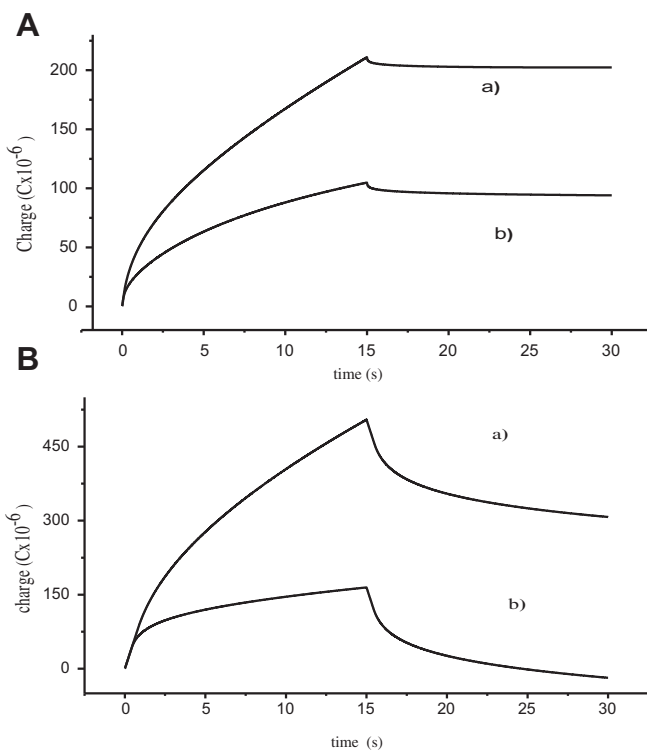


Fig. 4. Chronocoulomograms recorded for (A) p-(AHNSA)/GCRDE and (B) 181 $\mu\text{g cm}^{-2}$ platinum loaded p-(AHNSA)/GCRDE in: (a) oxygen saturated 0.5 M H_2SO_4 solution, (b) argon saturated 0.5 M H_2SO_4 solution.

where n is the number of electrons transferred, F is the Faraday constant ($96,484 \text{ C mol}^{-1}$), A is the geometric area of the glassy carbon electrode (0.0707 cm^2), C_0 is concentration of oxygen in oxygen saturated 0.5 M H_2SO_4 ($1.03 \times 10^{-3} \text{ mol dm}^{-3}$), D is the diffusion coefficient of oxygen in 0.5 M H_2SO_4 ($2.1 \times 10^{-5} \text{ cm}^2 \text{ s}^{-1}$).

From the slope of the curve obtained by plotting Q against $t^{1/2}$, the numbers of electrons (n) involved in the oxygen reduction processes are calculated to be 1.8 at the p-(AHNSA)/GCRDE and 3.8 at platinum loaded p-(AHNSA)/GCRDE.

3.2.3. Rotating disk electrode studies

The inset in Fig. 5 shows the linear sweep voltammograms for the reduction of oxygen saturated in 0.5 M H_2SO_4 at the p-(AHNSA)/GCRDE (normalized to the geometric area of the GCRDE $A = 0.0707 \text{ cm}^2$). The onset potential is at -0.2 V . The reduction of oxygen saturated in 0.5 M H_2SO_4 is also investigated at platinum loaded p-(AHNSA)/GCRDE for different platinum loadings at various rotations (from 0 to 3200 rpm). As a typical example, the complete analysis for the 181 μg platinum loading is given below.

Fig. 5 shows the linear sweep voltammograms recorded for oxygen reduction in 0.5 M H_2SO_4 solution saturated with oxygen at 181 μg platinum loaded p-(AHNSA) at different rotational speeds.

In the figure, it is clearly seen that the oxygen reduction reaction occurs at 0.5 V which corresponds with the four electron reduction path way of O_2 to H_2O on the platinum. This confirms that the oxygen reduction reaction is catalyzed by the presence of the platinum on the polymer [20,29].

The current density vs. potential curves for rotational speeds of $\omega = 100, 400, \text{ and } 1600 \text{ rpm}$ with all platinum loadings are shown in Fig. 6. The current densities platinum loadings are increasing with increasing rotational speeds except the current density for low platinum loadings. For low platinum loadings, the responses are found to be less dependent on the rotational rate suggesting that

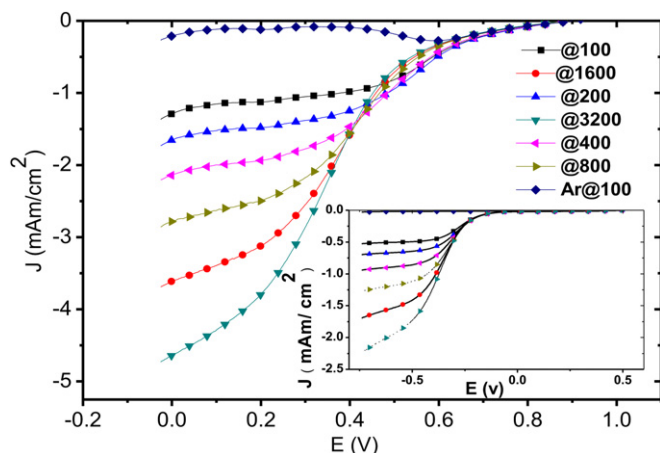


Fig. 5. Current density vs. potential plot for the reduction of oxygen saturated in 0.5 M H_2SO_4 at platinum modified p-(AHNSA)/GCRDE ($181 \mu\text{g Pt cm}^{-2}$) at different rotational speeds at scan rate of 10 mV s^{-1} , at 25°C . Inset: current density vs. potential curves for the reduction of oxygen saturated in 0.5 M H_2SO_4 at p-(AHNSA)/GCRDE, under similar condition.

the adsorption step partially controls the rate of the overall reduction reaction [5].

3.3. Analysis of the data

The overall current density can be described as:

$$\frac{1}{j} = \frac{1}{j_k} + \frac{1}{j_d} \quad (3)$$

and

$$j_d = 0.20nFCD^{2/3}v^{-1/6}\omega^{1/2} = nB\omega^{1/2} \quad (4)$$

where n is the number of electrons transferred in the reaction, F is the Faraday constant, A is the geometric area of the electrode, C is the concentration of oxygen in the solution ($1.03 \times 10^{-3} \text{ mol dm}^{-3}$), D is the diffusion coefficient ($2.1 \times 10^{-5} \text{ cm}^2 \text{ s}^{-1}$) in 0.5 M H_2SO_4 , v is the kinematic viscosity of ($1.075 \times 10^{-2} \text{ cm}^2 \text{ s}^{-1}$), and ω is the electrode rotational speed (rpm). Using the relation, in plot of equations (4) and (5) the inverse of the current density at constant potential vs. $\omega^{-1/2}$ gives the inverse of kinetic current density (j_k) and Levich constant (B) as an intercept and slope respectively. From the slope of the curve, the Levich constant (B) is calculated to be $0.0322 \text{ mA cm}^{-2} (\text{rpm})^{-1/2}$. To determine the number of electrons transferred in the reaction, the overall current density (j^{-1}) is plotted against the square root of the angular velocity ($\omega^{-1/2}$) resulting in Koutecky–Levich plot (K–L plot). Fig. 7 shows the K–L plot of j^{-1} vs. $\omega^{-1/2}$ (with data taken from Fig. 5) at different electrode potentials. Straight lines yielded $n \approx 4$ over a wide potential range of 0.18–0.35 V for platinum loading of $181 \mu\text{g}$ (Table 1). This value is in agreement with the value obtained from the chronocoulometric study and corresponds to the oxygen reduction reaction as ($\text{O}_2 + 4\text{H}^+ + 4\text{e}^- \rightarrow 2\text{H}_2\text{O}$), the direct four electron reduction of O_2 to H_2O . Similar results obtained for most platinum loaded polymers [5,11].

The inset in the same figure shows the K–L plot of the p-(AHNSA)/GCRDE at different electrode potential. Straight and parallel lines are obtained with slope remaining constant in the potential range of -0.40 to -0.50 V [28]. The slope of the Koutecky–Levich plot of j^{-1} vs. $\omega^{-1/2}$ yielded $n \approx 2$ [3].

In Fig. 8 K–L plot of (A) p-(AHNSA)/GCRDE and (B) platinum loaded p-(AHNSA)/GCRDE at two different potential is compared

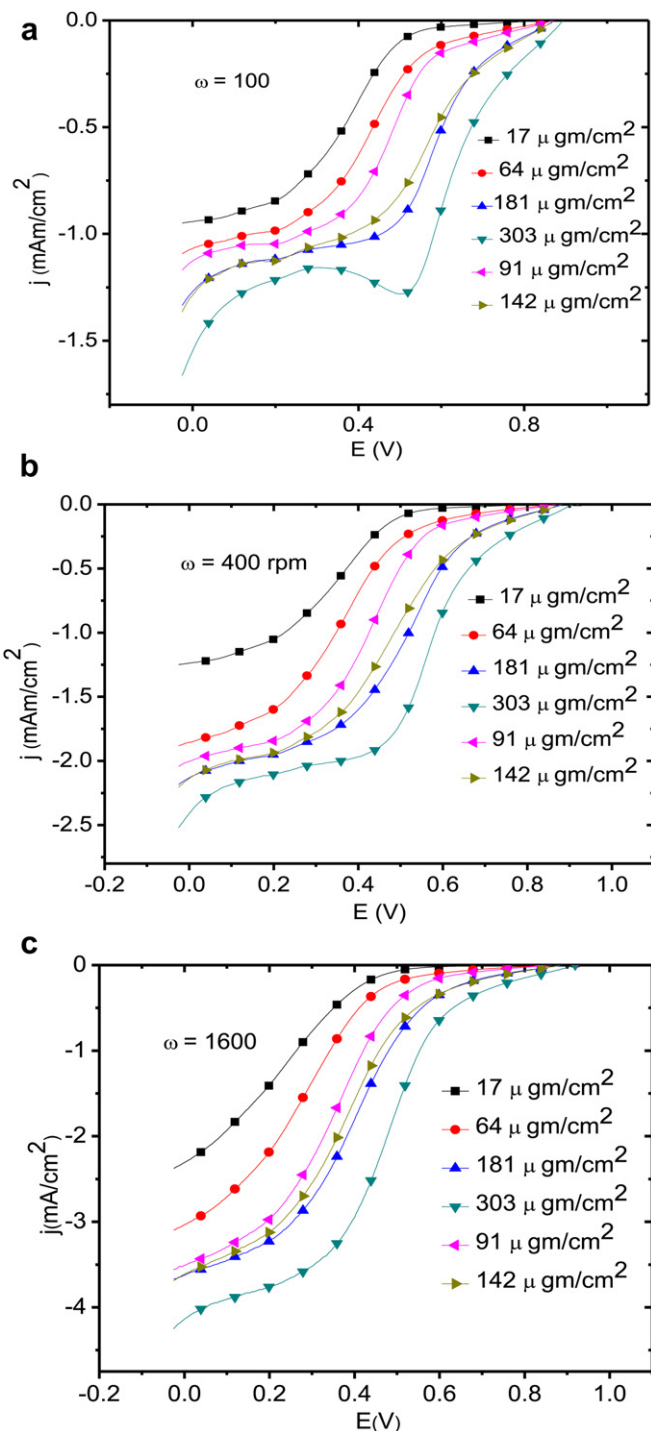


Fig. 6. Current–potential curves for the reduction of oxygen saturated in 0.5 M H_2SO_4 at p-(AHNSA)/GCRDE loaded with different amounts of platinum (17 – $303 \mu\text{g cm}^{-2}$) at different rotational speeds: (a) $\omega = 100$, (b) $\omega = 400$ and (c) $\omega = 1600 \text{ rpm}$. Scan rate: 10 mV s^{-1} ; at 25°C .

with the theoretical two and four electron K–L plot. The plot of p-(AHNSA)/GCRDE is parallel and has the same slope with theoretical plot of 2 electron path while for platinum loaded p-(AHNSA)/GCRDE is parallel and had the same slope with theoretical plot of 4 electron path way, which is consistent with calculated number of electrons from equation (4) and from the calculation of the chronocoulometric plot (Table 1).

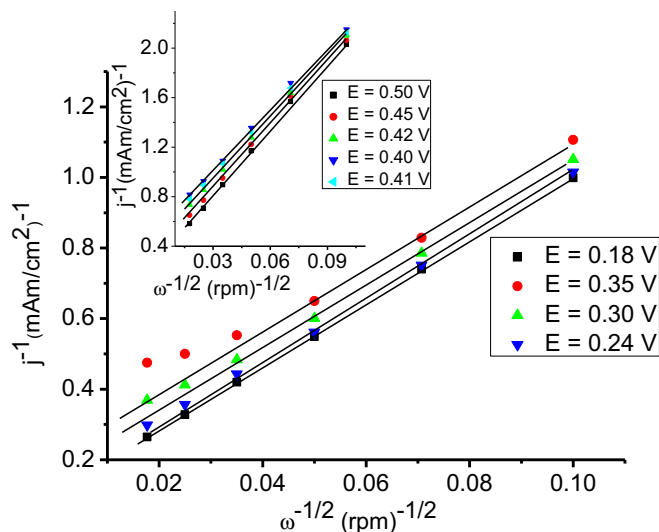


Fig. 7. Koutecky–Levich plot for the reduction of oxygen in oxygen saturated 0.5 M H_2SO_4 at platinum loaded ($181 \mu\text{g cm}^{-2}$) p-(AHNSA)/RDGCE at different potentials. Scan rate: 10 mV s^{-1} and temperature 25°C . Inset: Koutecky–Levich plot of oxygen reduction in oxygen saturated 0.5 M H_2SO_4 at p-(AHNSA)/p-(AHNSA)/RDGCE under similar conditions.

From the Koutecky–Levich plot (Fig. 7), the intercept at the origin ($\omega \rightarrow \infty$) gives the inverse of the kinetic current density j_k . The dependence of the kinetic current density on the overpotential is shown in equation (5) below.

$$\frac{1}{j_k} = \frac{1}{j_l} + \frac{1}{j_0} \exp\left(\frac{|\eta|}{b}\right) \quad (5)$$

As can be seen from Fig. 9, for high over voltage the quantity j_k^{-1} approaches to j_l^{-1} (the limiting current density).

The Tafel slope and exchange current density is calculated using the relation:

$$\eta = E - E_{\text{eq}} = -b \left\{ \ln \frac{j_l}{j_0} + \ln \left[\frac{j_k}{j_l - j_k} \right] \right\} \quad (6)$$

Plotting η or E vs. $\ln[j_k/j_l - j_k]$ gives $-b$ as a Tafel slope and the intercept at the origin is used to calculate j_0 (exchange current density) using the known limiting current density (Table 1) [28,30].

The Tafel slope and the exchange current density calculated from the plot of E vs. $\ln[j_k/j_l - j_k]$, shown in Fig. 10, for platinum loading of $181 \mu\text{g cm}^{-2}$ are given in Table 1. The Tafel slope varies from a value of about 35 mV dec^{-1} for lowest platinum loading to 106 mV dec^{-1} values to higher amount of platinum loading. This could be ascribed to Temkin and Langmuirian adsorption isotherms

Table 1

Kinetic parameters for the oxygen reduction reaction at p-(AHNSA)/GCRDE and platinum loaded p-(AHNSA)/GCRDE at different platinum loadings.

Pt loading ($\text{W}/\mu\text{g cm}^{-2}$)	Total number of electrons (n) ^a	Limiting current density ($j_l/\text{mA cm}^{-2}$)	Tafel slope ($b/\text{mV decade}^{-1}$)	Exchange current density ($j_0/\text{mA cm}^{-2}$)
0	1.8	3.69	44	4.82×10^{-4}
17	3.6	4.10	35	5.21×10^{-3}
64	3.5	8.20	70	7.03×10^{-3}
91	3.6	11.23	71	1.77×10^{-3}
142	3.1	11.70	71	1.77×10^{-3}
181	3.4	10.45	83	1.63×10^{-3}
303	3.7	27.13	106	1.40×10^{-3}

^a Average of the number of electrons calculated at different electrode potentials.

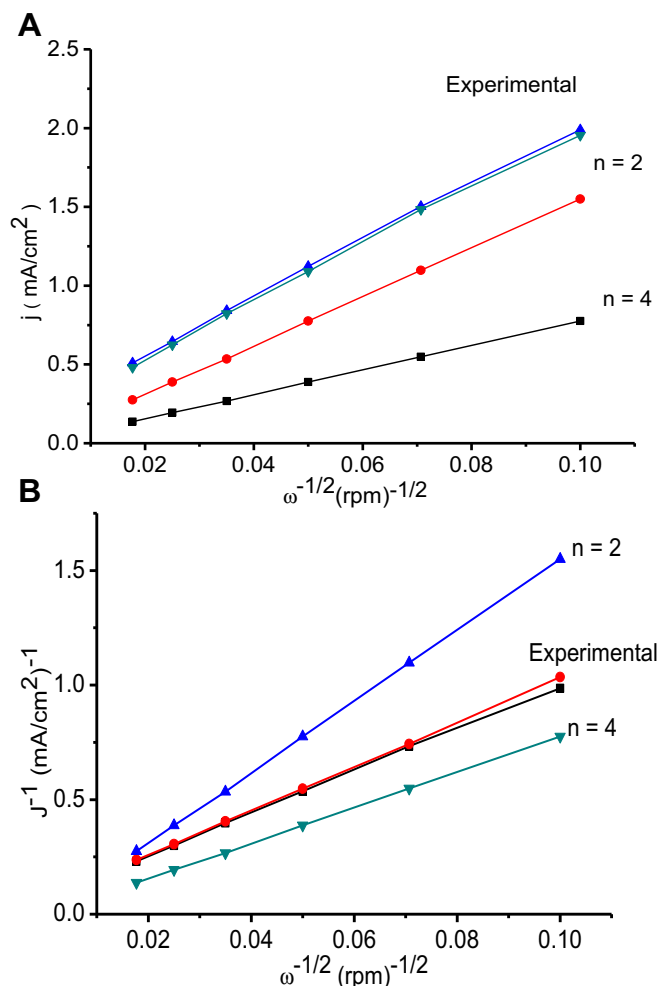


Fig. 8. Koutecky–Levich plot for the reduction of oxygen in oxygen saturated 0.5 M H_2SO_4 at (A) p-(AHNSA)/RDGCE at potentials of 0.663 and 0.603 V, (B) platinum loaded ($181 \mu\text{g cm}^{-2}$) p-(AHNSA)/RDGCE at potentials of 0.014 and 0.057 V.

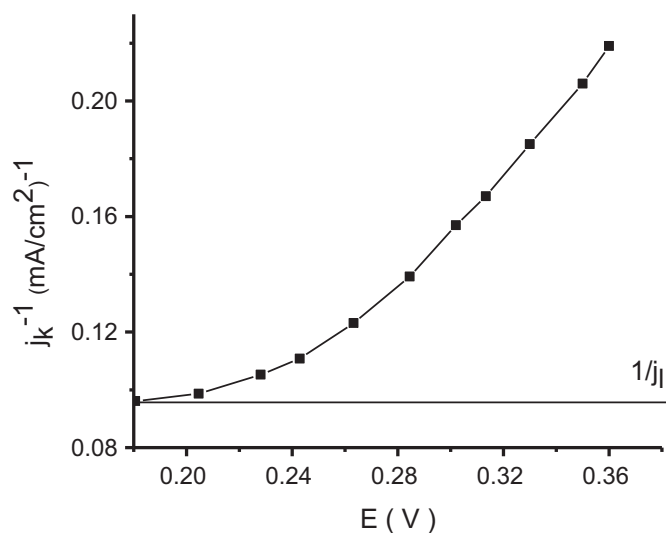


Fig. 9. Plot of j_k^{-1} vs. E for the reduction of oxygen in oxygen saturated 0.5 M H_2SO_4 at platinum ($181 \mu\text{g cm}^{-2}$) loaded p-(AHNSA)/RDGCE.

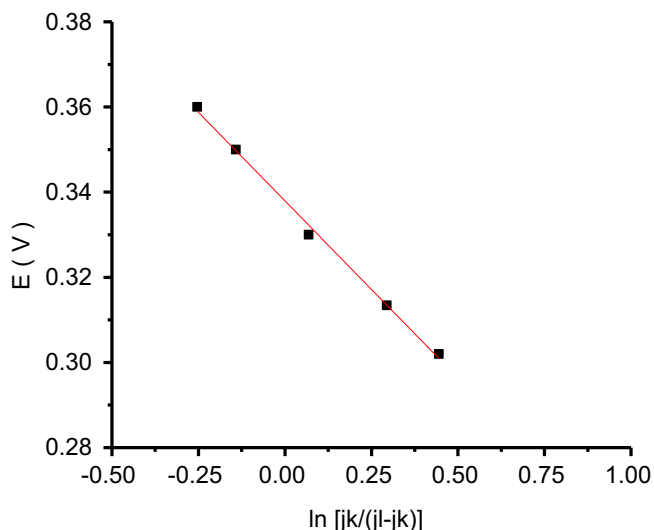


Fig. 10. Plot of potential E vs. $\ln[j_k/(j_1 - j_k)]$ for the reduction of oxygen in oxygen saturated 0.5 M H_2SO_4 ; at a platinum ($181 \mu g\ cm^{-2}$) loaded p-(AHNSA)/RDGCE. Inset: plot of potential E vs. $\ln[j_k/(j_1 - j_k)]$ for the reduction of oxygen in oxygen saturated 0.5 M H_2SO_4 at p-(AHNSA)/RDGCE under similar conditions.

respectively. One can also evaluate the exchange current density from the intercept of the plot of E vs. $\ln[j_k/(j_1 - j_k)]$. The result obtained for the exchange current density for platinum loading of $181 \mu g\ cm^{-2}$ is $1.63 \times 10^{-3} mA\ cm^{-2}$ which is much higher than the limiting current density by a factor of 10^3 . Similarly, the p-(AHNSA) modified electrode has an exchange current density of $4.82 \times 10^{-4} mA\ cm^{-2}$ which is 10^4 times higher than the limiting current density [31–34].

4. Conclusion

The electropolymerized p-(AHNSA)/GCRDE and the platinum loaded p-(AHNSA)/GCRDE were used to study their electrocatalytic activities towards oxygen reduction reaction. The platinum loaded p-(AHNSA)/GCRDE was found to change the oxygen reduction reaction path from 2 in p-(AHNSA)/GCRDE to 4 electrons. The onset potential was significantly increased with increasing platinum loadings from 0 to $303 \mu g$. Kinetic parameters like j_0 , j_1 and Tafel slope were evaluated. Good catalytic activity was observed with low platinum loadings on p-(AHNSA)/GCRDE.

References

- [1] S.A. Kumar, S.M. Chen, J. Mol. Catal. A Chem. 278 (2007) 244–250.
- [2] H. Park, T.G. Kwon, D.S. Park, Y.B. Shim, Bull. Korean Chem. Soc. 27 (11) (2006) 1763–1768.
- [3] V.G. Khomenko, V.Z. Barsukov, A.S. Katashinskii, Electrochim. Acta 50 (2005) 1675–1683.
- [4] B.W. Jensen, O.W. Forsyth, D.R. Farlane, Science 321 (2008) 671–674.
- [5] C. Coutanceau, M.J. Napporn, C. Lamy, Electrochim. Acta 46 (2000) 579–588.
- [6] E.K. Lai, P.D. Battic, F.P. Orfino, E. Simon, S. Holdcroft, Electrochim. Acta 44 (1999) 2559–2569.
- [7] K.M. Kost, D.E. Bartak, B. Kaze, T. Kuwane, Anal. Chem. 60 (1988) 2379–2384.
- [8] Q. Yang, Y. Wang, H. Nakano, S. Kuwabata, Polym. Adv. Technol. 16 (2005) 759–763.
- [9] B. Rajesh, K.R. Thampi, J.M. Bonard, Electrochem. Solid State Lett. 7 (2004) A404–A407.
- [10] S. Holdcroft, B.L. Funt, J. Electroanal. Chem. 240 (1988) 89–103.
- [11] P. Gajendran, S. Vijayanand, R. Saraswathi, J. Electroanal. Chem. 601 (2007) 132–138.
- [12] Z.D. Wei, S.H. Chan, L.L. Li, H.F. Cai, Z.T. Xia, C.X. Sun, Electrochim. Acta 50 (2005) 2279–2287.
- [13] T. Okada, H. Satou, M. Yuasa, Langmuir 19 (2003) 2325–2332.
- [14] T. Okada, J. Dale, Y. Ayato, O.A. Asbjørnsen, M. Yuasa, I. Sekine, Langmuir 15 (1999) 8490–8496.
- [15] T. Okada, Y. Ayato, J. Dale, M. Yuasa, I. Sekine, O.A. Asbjørnsen, Phys. Chem. Chem. Phys. 2 (2000) 3255–3261.
- [16] M. Weissmann, C. Coutanceau, P. Brault, J.M. Leger, Electrochem. Commun. 9 (2007) 1097–1101.
- [17] H. Yano, J. Inukai, H. Uchida, M. Watanabe, P.K. Babu, T. Kobayashi, J.H. Chung, E. Oldfield, A. Wieckowski, Phys. Chem. Chem. Phys. 8 (2006) 4932–4939.
- [18] J. Shan, P.G. Pickup, Electrochim. Acta 46 (2000) 119–125.
- [19] Z.G. Estephan, L. Alawieh, L.I. Halaoui, J. Phys. Chem. C 111 (2007) 8060–8068.
- [20] S. Shanmugam, A. Gedanken, J. Phys. Chem. C 113 (2009) 18707–18712.
- [21] W. Chen, J. Kim, S. Sun, S. Chen, J. Phys. Chem. C 112 (2008) 3891–3898.
- [22] B.E. Hayden, D. Pletcher, J.P. Suchsland, L.J. Williams, Phys. Chem. Chem. Phys. 11 (2009) 9141–9148.
- [23] I. Dutta, M.K. Carpenter, M.P. Balogh, J.M. Ziegelbauer, T.E. Moylan, M.H. Atwan, N.P. Irish, J. Phys. Chem. C 114 (2010) 16309–16320.
- [24] Y. Zhang, Q. Huang, Z. Zou, J. Yang, W. Vogel, H. Yang, J. Phys. Chem. C 114 (2010) 6860–6868.
- [25] M. Amare, W. Lakew, S. Admassie, Anal. Bioanal. Electrochem. 3 (2011) 365–378.
- [26] S.M. Alia, G. Zhang, D. Kisailus, D. Li, S. Gu, K. Jensen, Y. Yan, Adv. Funct. Mater. 20 (2010) 3742–3746.
- [27] H. Li, G. Sun, N. Li, S. Sun, D. Su, Q. Xin, J. Phys. Chem. C 111 (2007) 5605–5617.
- [28] A.J. Bard, L.R. Faulkner, Electrochemical Methods, Fundamental and Applications, Wiley, New York, 2001, pp. 341–344.
- [29] C.V. Rao, B. Viswanathan, J. Phys. Chem. C 114 (2010) 8661–8667.
- [30] M.J. Croissant, T. Napporn, J.M. Leger, C. Lamy, Electrochim. Acta 43 (1998) 2447–2457.
- [31] D.B. Sepa, M.V. Vojnovic, L.J.M. Vracar, A. Damjanovic, Electrochim. Acta 36 (1986) 91–96.
- [32] D.B. Sepa, A. Damjanovic, Electrochim. Acta 25 (1980) 1491–1496.
- [33] D.B. Sepa, M.V. Vojnovic, A. Damjanovic, Electrochim. Acta 26 (1981) 781–793.
- [34] J. O' M Bockris, A.K.N. Reddy, M.G. Aldeco, Modern Electrochemistry. 2A, second ed., Kluwer Academic, Plenum Publishers, New York, 1998, pp. 1056–1058.